Available online at www.sciencedirect.com
ScienceDirect
Trans. Nonferrous Met. Soc. China 29(2019) 791−798
Transactions of Nonferrous Metals Society of China
www.tnmsc.cn

Electrocaloric behavior of $Ba_{0.85}Ca_{0.15}Zr_{0.1}Ti_{0.88}Sn_{0.02}O_3$ cement composites

P. SURESH, P. MATHIYALAGAN, K. S. SRIKANTH

School of Mechanical Engineering, Galgotias University, Greater Noida, Uttar Pradesh, 201306, India

Received 22 June 2018; accepted 28 December 2018

Abstract: A thrust for looking multifunctional materials for applications in civil engineering structures has attracted interest among researchers across the globe. Cement based $Ba_{0.85}Ca_{0.15}Zr_{0.1}Ti_{0.88}Sn_{0.02}O_3$ (BCZT−Sn) composites were prepared for electrocaloric applications with varying BCZT−Sn to cement ratio. Hysteresis loops showed some signature of saturation in cement composites. However, loops of pure sample were saturated due to its ferroelectric nature. Furthermore, these composites were explored for the first time in solid state refrigeration technology namely electrocaloric effect (ECE). Peak electrocaloric performance shows an adiabatic temperature changes of 0.71, 0.64 and 0.50 K and isothermal entropy changes of 0.86, 0.80 and 0.65 J/(kg·K) for BCZT−Sn, 10% and 15% cement composites, respectively, under application of 0−29 kV/cm electric field. The adiabatic temperature change in cement based composites is comparable with that of the BCZT−Sn ferroelectric ceramics. Furthermore, the dielectric constant (ε_r) of composites with different ceramic contents at room temperature reveals that dielectric constant increases with an increase in BCZT−Sn proportion in composites. These cement based BCZT−Sn composite materials may be used in solid state refrigeration as they are fairly competitive with the pristine sample.

Key words: electrocaloric behavior; cement composites; dielectric; entropy

1 Introduction

In order to have more efficient and functional buildings, there is a thrust of multi-functional properties in structural materials. Cement materials are the largely used building materials in structural engineering [1,2]. After many decades of use of concrete structures and because of the living environmental effect, the building structures may get affected. Therefore, it becomes quite arduous to immediately sense the damaged structure [3]. In this context, developing intelligent structures with features like self-inspection is the need of the hour [2−4]. Apart from safety, reduction of carbon and conservation of energy are also of prime importance. These difficulties paved the way for looking for new functionalities in building materials.

In this context, piezoelectric composite materials look promising to overcome the functional deficiencies. These materials have the potential to be used for sensors because of their piezoelectric properties [5,6]. The piezoelectric composite with cement matrix can be used to develop sensors that are really smart in real time structural health monitoring [2,7,8]. The incorporation of piezoelectric ceramic in cement significantly enhances the functionality of structural materials [9]. It is thus very interesting to explore such area for various applications.

Amongst many articles exploring such area, lead zirconate titanate (PZT)-based cement composite is one of them [10−13]. Researchers in Refs. [2,6,11] prepared PZT−cement composites using normal mixing and spreading methods and reported slightly higher electromechanical coefficient and piezoelectric strain factor than 0−3 PZT-polymer composites with a similar content of ceramics (PZT). However, these composites are made using PMN or PZT that are lead based and are of carcinogen nature which is main cause of cancer and other serious health hazards [14,15]. Therefore, due to environmental concerns, a demand has been increasing to eliminate toxic lead for these material systems.

In this context, $BaTiO_3$ (BT, lead-free) based cement composites were prepared by RIANYOI et al [16] and the influence of ceramic content on the electromechanical coupling coefficient of cement based composites was studied. Apart from the civil engineering applications, these cement based composites were

Corresponding author: P. SURESH; Tel: +91-8130568273; E-mail: psuresh2730@gmail.com
DOI: 10.1016/S1003-6326(19)64989-7

explored for the first time in solid state refrigeration technology. There are several solid state refrigeration technologies which are under research like magnetoelectric, thermoelectric and electrocaloric refrigeration. Among these listed techniques, the electrocaloric refrigeration technique has many advantages. The electrocaloric effect (ECE) is a very good phenomenon in ferroelectric materials in which a material shows a reversible temperature change under the application of an electric field in adiabatic conditions [17−19]. A large electrocaloric effect may provide an efficient way to realize such solid state cooling devices for a broad range of applications including temperature regulation for sensors, electronic devices, and on-chip cooling etc.

The first study in this area was done in Rochelle salt in 1930s [17−19]. After more than thirty years of silence (since 1960s), the exploration paved the way for new type of refrigeration system using ferroelectric materials. Thereafter, abundant data have been reported in many kinds of ferroelectric materials like bulk materials, thin films, thick films and polymers [20,21]. A large ECE could be seen in thin film materials due to their ability to sustain higher breakdown field. In this direction, a large ECE of 12 K at 226 °C has been reported in $PbZr_{0.95}Ti_{0.05}O_3$ thin films. Although large ECE is achieved in thin film, the heat extraction capacity is always lower than that of the ceramics. Therefore, the research on bulk electrocaloric materials is still a subject of interest. For instance, a large ECE of 4.5 K at 38 °C has been reported in $BaZr_xTi_{1-x}O_3$ bulk ceramics at temperatures close to the first order phase-transition [22]. Large ECE value of 1.64 K was observed in $BaHf_xTi_{1-x}O_3$ compositions with x=0.05 [23]. In this context, the family of barium titanate based ceramics have been extensively investigated as they show excellent ferroelectric behavior [24,25]. In this direction, it was reported that the incorporation of Zr and Ca in $BaTiO_3$ system enhances the pyroelectric, ferroelectric and piezoelectric properties when fabricated in the morphotropic phase boundary (MPB) [17]. Therefore, barium calcium zirconium titanate (BCZT) ceramics have been widely investigated. BCZT based ceramics are potential lead-free materials suitable for solid state cooling as they show low electric field saturation [18,24,26]. Recently, KADDOUSSI et al [27,28] have found that adding Sn element to BCZT decreases the phase transition temperature with a large EC responsivity of 26.2 mK·cm/kV.

However, the ECE effect in cement based composites has not been explored till date. Therefore, the present work focused on BCZT−Sn solid solution using cement as the filler for the electrocaloric refrigeration applications. Furthermore, the ferroelectric hysteresis loops of cement composites were also discussed in detail which are important parameters to find the ECE. All the previous reports indicated low content of ceramics in the composite which resulted in round loops due to high losses associated with larger fraction of cement. Therefore, cement based composites with higher fraction of ferroelectric ceramic were prepared and studied.

2 Experimental

A conventional solid state fabrication route was used to prepare $Ba_{0.85}Ca_{0.15}Zr_{0.1}Ti_{0.88}Sn_{0.02}O_3$ (BCZT−Sn) ceramics. Reagent grade (>99% pure) powders of $BaCO_3$, CaO, ZrO_2, TiO_2 and $SnCl_2$ were used as the starting precursors.

The starting precursor powders were mixed according to stoichiometric ratio with 2% Sn (mole fraction). Initially, these materials were ball milled using acetone as the wetting agent to attain physical homogeneity. The mixture powders were calcined at 1350 °C for 6 h after drying. The resultant mixture was compressed under a uniaxial pressure of 392 MPa and made into pellets of 12 mm × 0.9 mm (diameter× thickness). Then, the pellets were sintered by conventional technique at 1400 °C for 6 h. X-ray diffraction technique was performed to confirm the formation of single phase.

To prepare BCZT−Sn cement composites, the calcined powder was mixed with varying compositions of 10% and 15% ordinary Portland cement by mass fraction. Water was then added to the resultant mixture (0.25 mL) according to a certain water/cement ratio and subsequently poured into the mould. The mould specimens were cured for 28 d in water to obtain hardness. After curing, specimen surfaces of composite were polished to obtain disk shape with 12 mm in diameter and 0.9 mm in thickness.

The morphology of the surface was characterized by scanning electron microscopy (SEM). Archimedes principle was employed to determine the density of these samples. For measuring hysteresis loop (P−E), the flat surfaces of the specimens were coated with silver paste to form electrical contacts. The samples were subjected to bipolar electrical field (50 Hz) to obtain polarization (P)−electric field (E) loops at different magnitudes of electric fields and temperatures using a modified Sawyer Tower circuit. The dielectric properties of the composites were measured by using an Agilent precision impedance analyzer. The dielectric constant (ε_r) was evaluated from Eq. (1) as follows:

$$\varepsilon_r = C_p t/(\varepsilon_0 A) \quad (1)$$

where C_p denotes capacitance of the sample, t is the thickness, A is area of electrode and ε_0 is the free space

permittivity (8.854×10^{-12} F/m).

3 Results and discussion

3.1 Microstructural characterization

The XRD pattern of BCZT−Sn sample is depicted in Fig. 1, which confirms the formation of single phase as there are no unidentified peaks related with secondary phase. The sharpness of X-ray diffraction peaks indicates good homogeneity and crystallinity of sample.

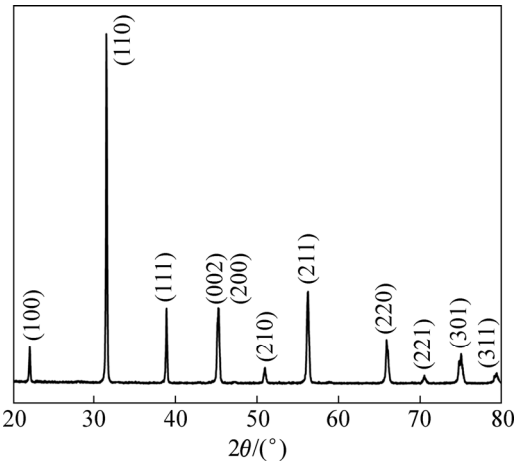

Fig. 1 X-ray diffraction pattern for calcined BCZT−Sn powder sample

Figure 2(a) shows the SEM micrograph of sintered BCZT−Sn ceramics. The surface of the sample was found to be free from any major porosity or anomaly. Further, the density of the sample was found to be 5.6 g/cm^3 using Archimedes principle, which was ~95% of the theoretical density. This confirms the high dense structure due to closely packed grains. However, the SEM images of cement composite show some pores which are formed due to the inclusion of cement. The microstructures of cement based ferroelectric composites are shown in Figs. 2(b) and (c). The density of the cement based composite was found to be 4.5 and 4.2 g/cm^3 using Archimedes principle for 10% and 15% cement, respectively, which reveals that there are more pores in the cement based composites compared with BCZT−Sn sintered ceramic pellet.

3.2 Hysteresis characteristics

In order to further investigate the hysteresis characteristics of BCZT−Sn ceramics and the cement based composites, *P*−*E* hysteresis loops of BCZT−Sn and cement−(BCZT−Sn) composites were recorded at varying temperatures and a constant frequency of 50 Hz as shown in Figs. 3(a), (b) and (c). The BCZT family of ceramics shows saturation at low electric field and belongs to low-field actuator materials [18,26]. This leads to low temperature change capacity in similar class

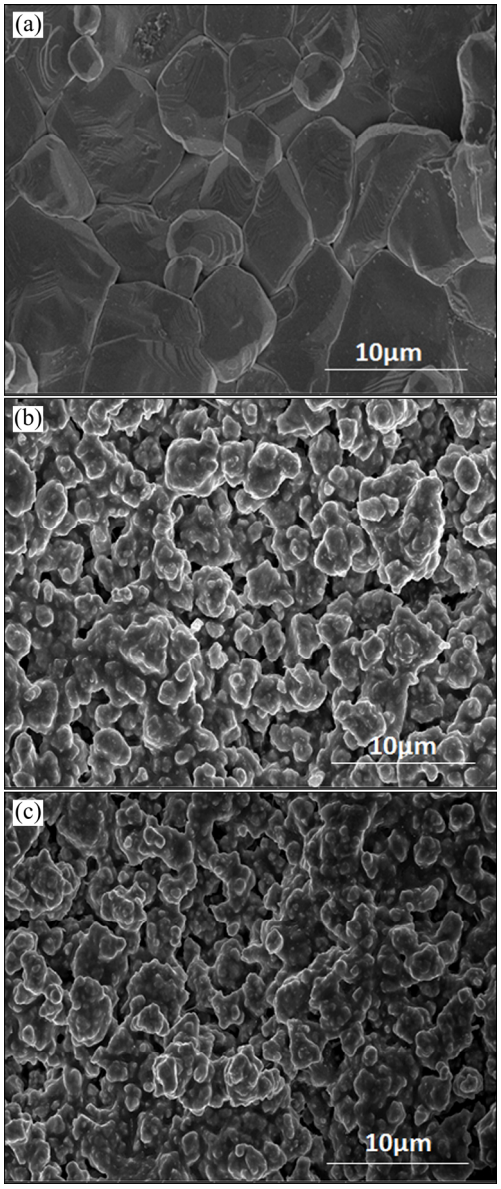

Fig. 2 SEM micrographs of pure BCZT−Sn sample (a), 90% (BCZT−Sn)−10% cement composites (b) and 85% (BCZT−Sn)−15% cement composites (c)

of ferroelectric ceramics. However, the addition of Sn can enhance the saturation polarization (P_{max}) and the polarization gradient $\partial P/\partial T$. In this direction, well sintered BCZT ceramics with 2% Sn doping resulted in the highest saturation polarization of 17.3 μC/cm^2 (as shown in Fig. 3(a)) compared with BCZT where P_{max} is obtained as 14 μC/cm^2 at 303 K [29,30]. Further, adding Sn decreases the ferroelectric properties [29].

Therefore, the 2% Sn doped BCZT ceramics was selected for the present investigation. Furthermore, the cement composites were made by normal mixing and pressing. The composites showed fair density and polarization. To study the polarization behavior, the *P*−*E* loops of the cement based composites (10% and 15%

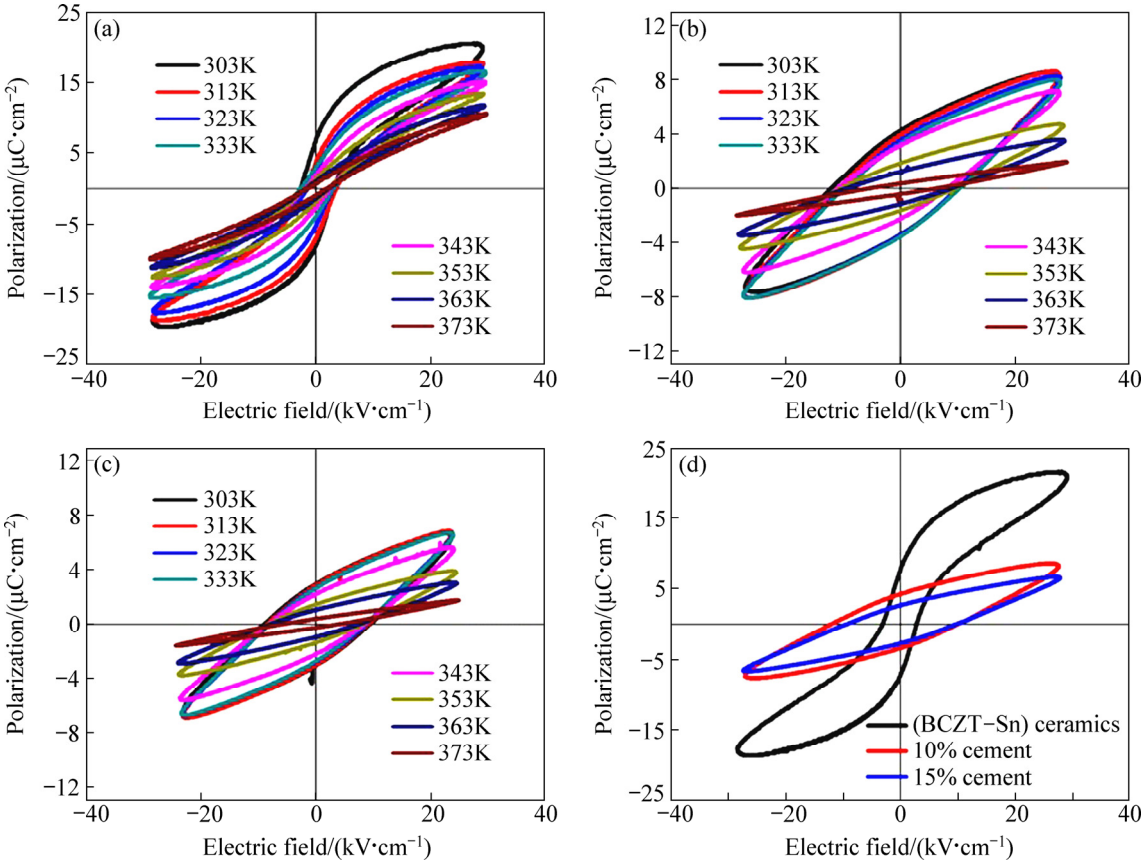

Fig. 3 *P*−*E* hysteresis loops of pure BCZT−Sn (a), 10% cement composite (b) and 15% cement composite (c) measured at different temperatures, and comparison of *P*−*E* loops at room temperature (d)

cement by mass fraction in BCZT−Sn) are depicted in Figs. 3(b) and (c), respectively.

It is important to note that due to porous microstructure in cement composites, *P*−*E* loops are not completely saturated when compared to BCZT−Sn ceramics. However, the loops of BCZT−Sn cement composites have shown some signature of saturation. Figure 3(d) shows the variation of polarization at room temperature for all the investigated samples. The hysteresis characteristics like remnant polarization and saturation polarization decrease with the inclusion of cement particles in BCZT−Sn ferroelectric ceramics as shown in Fig. 3(d). BCZT−Sn has a saturation polarization of 17.3 μC/cm^2 which reduces to 8.20 and 6.90 μC/cm^2 with addition of 10% and 15% cement to BCZT−Sn ceramics, respectively [29,30]. This reduction in hysteresis parameters owes to the fact that the samples exhibit lower density. This may also be attributed to the fact that due to the losses associated with cement ionic content, completely saturated loops were not obtained [30−35].

The BCZT−Sn is a ferroelectric material; hence, higher BCZT−Sn concentration in the composites should have higher P_r and P_{max}. Moreover, the *P*−*E* loops of composites are not saturated due to the presence of a non-ferro electric/piezoelectric layer of cement between the BCZT−Sn particles. The isolated ceramic particles increase with higher cement volume fraction in the composite. In the case of ferroelectric cement composites, the applied electric field (E) on the ceramic particles can be given as

$$E=\frac{3(\varepsilon_r'/\varepsilon_r)E_0}{[1+2(\varepsilon_r'/\varepsilon_r)]-V[1-(\varepsilon_r'/\varepsilon_r)]} \quad (2)$$

where ε_r', V and E_0 are relative permittivity of the cement matrix, volume fraction of the ferroelectric ceramic and externally applied electric field, respectively. ε_r', ε_r and E_0 are constant, therefore, E depends only on the ceramic volume fraction. The reduction in net polarization can be ascribed to the fact that adding cement generates an internal stress between ferroelectric ceramic and cement which consequently leads to the reduction in net polarization as shown schematically in Fig. 4 [36].

It is shown that under the application of electric field, the ferroelectric cement gets strained due to ferroelectric switching which is associated with 180° domain rotation as depicted in Fig. 4(a). However, the

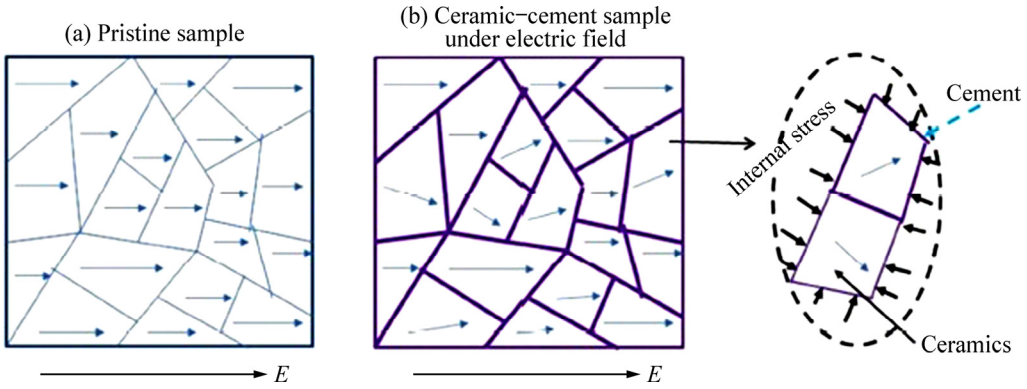

Fig. 4 Pure ceramic (a) and cement composite (b) under influence of electric field

addition of cement generates internal stress which consequently leads to internal clamping of domains as shown in Fig. 4(b). Such phenomenon has been well explained in Ref. [36].

3.3 Electrocaloric properties

In order to evaluate the electrocaloric properties of BCZT−Sn bulk ceramics, *P*−*E* loops were recorded for every 10 K interval from 303 to 373 K. From the *P*−*E* loops plots, the maximum polarization data (P_{max}) are extracted from their upper branches which were plotted against operating temperature. From these values, the *P*−*T* graph was plotted and further polynomial fitting with goodness of fit R^2=0.99 was done to obtain large number of data (close to 100). These obtained data were further utilized to calculate electrocaloric temperature change (ΔT) and isothermal entropy change (ΔS) as shown in Figs. 5(a) and (b), respectively.

It is reported that the incorporation of 2% Sn into the pure BCZT ceramics increases both P_{max} and polarization gradient with respect to temperature which is capable of exhibiting pronounced caloric effect [29]. The Maxwell's relation $(\partial P/\partial T)_E=(\partial S/\partial E)_T$ was used to estimate the adiabatic temperature change (ΔT) and isothermal entropy change (ΔS) using the following equations [19,26,37−39]:

$$\Delta T=-\frac{1}{\rho c_p}\int_{E_1}^{E_2}T\left(\frac{\partial P}{\partial T}\right)\mathrm{d}E \tag{3}$$

$$\Delta S=-\frac{1}{\rho}\int_{E_1}^{E_2}\left(\frac{\partial P}{\partial T}\right)\mathrm{d}E \tag{4}$$

where P represents polarization, E_1 and E_2 are the lower and higher electric field limits, respectively, c_p denotes the specific heat capacity of the material and ρ implies the density of the ceramics which was measured by employing Archimedes principle. The temperature dependent specific heat capacity is reported for BCZT ceramics which was used for estimating the EC effect [40].

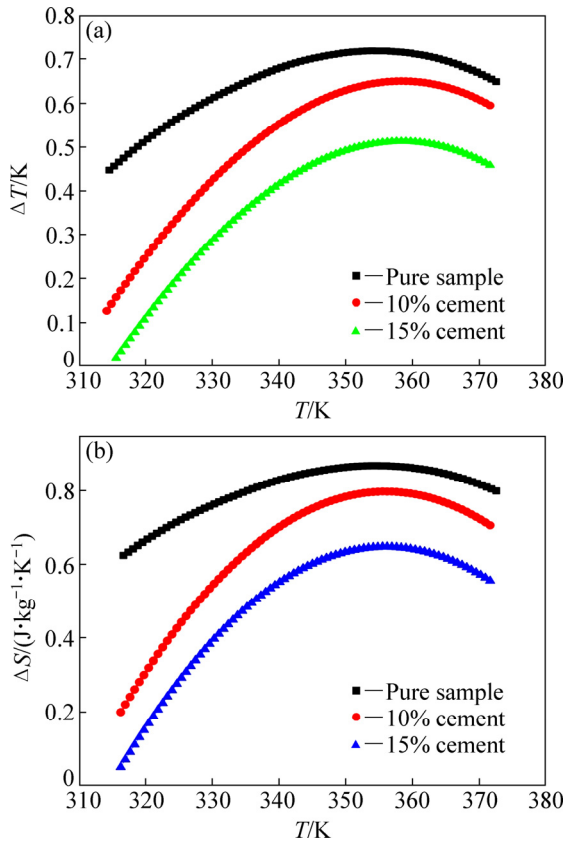

Fig. 5 Comparison plots showing electrocaloric effect (ΔT) (a) and isothermal entropy change (ΔS) (b) versus temperature (T) of BCZT−Sn ceramics and cement composites under same electric field

The specific heat capacity for cement composites is kept constant at all temperatures and estimated by employing rule of mixtures as shown:

$$(\rho c_p)_{\mathrm{com}}=V(\rho c_p)_{\mathrm{p}}+(1-V)(\rho c_p)_{\mathrm{c}} \tag{5}$$

where subscripts com, p and c represent composite, pure sample and cement, respectively, and V denotes the volume fraction.

Figure 5(a) provides more information about

the influence of ceramic/cement ratio in composites for electrocaloric cooling. The comparison of EC characteristics of BCZT−Sn, 10% cement and 15% cement composites, respectively versus material temperature under electric field of 29 kV/cm is plotted in Fig. 5(a). The pure sample (2% Sn doped) possess a maximum ΔT of 0.71 K at electric field of 29 kV/cm and 358 K.

This composition (2% Sn dopant) is the best composition to obtain a meliorated EC performance in BCZT-based ferroelectric materials. The maximum ΔT is achieved as a result of ferroelectric to paraelectric phase transition corresponding to tetragonal to cubic phase [19,41]. However, the adiabatic temperature changes of 0.64 and 0.50 K at 358 K were estimated for 10% and 15% cement composites, respectively. These values are quite significant and comparable with the other ferroelectric ceramics.

Only adiabatic temperature change does not provide sufficient information to predict the electrocaloric performance of a material. Another important parameter is isothermal entropy change (ΔS) which predicts the overall heat extraction capacity of a sample. Figure 5(b) displays ΔS as a function of temperature at a particular electric field of 29 kV/cm for all investigated samples. The pure sample (BCZT−Sn) gives a maximum ΔS of 0.86 J/(kg·K). The maximum entropy changes in cement composites with 10% and 15% cement by mass fraction in BCZT−Sn were found to be 0.78 and 0.64 J/(kg·K), respectively.

These estimated values are obviously lower than that of the pure BCZT−Sn sample. However, there are several advantages associated with cement based composites, such as (1) these composites can be fabricated without any sintering processes, (2) it is easy to cast them into any shape and size, (3) the product cost will be lower, and (4) it can be installed with cement structure for next generation energy efficient buildings.

3.4 Dielectric behavior

In order to have materials for caloric applications, the dielectric losses should be negligible. In this context, the dielectric properties of cement based composites were studied. The capacitances of BCZT−Sn and the cement composites were determined at various frequencies by utilizing impedance analyzer. The temperature dependent dielectric constant for the samples investigated was calculated from the obtained capacitance using Eq. (1). The dielectric constant of BCZT−Sn has a peak value of 6500 at phase transition measured at frequency of 1 kHz, as shown in Fig. 6(a). The dielectric constant for the BCZT−Sn−cement composites of 10% and 15% cement by mass fraction are depicted in Figs. 6(b) and (c), respectively.

It is observed that the dielectric constant increases with the increase in ceramic content in the composites. From these results, it is observed that all the samples are in agreement with previous studies which show increasing ε_r with the increase in ceramic particle content. Generally, the dielectric constant decreases with the increase in porosity in samples. The dielectric loss values (tan δ) for all the samples are also depicted in Figs. 6(a), (b) and (c).

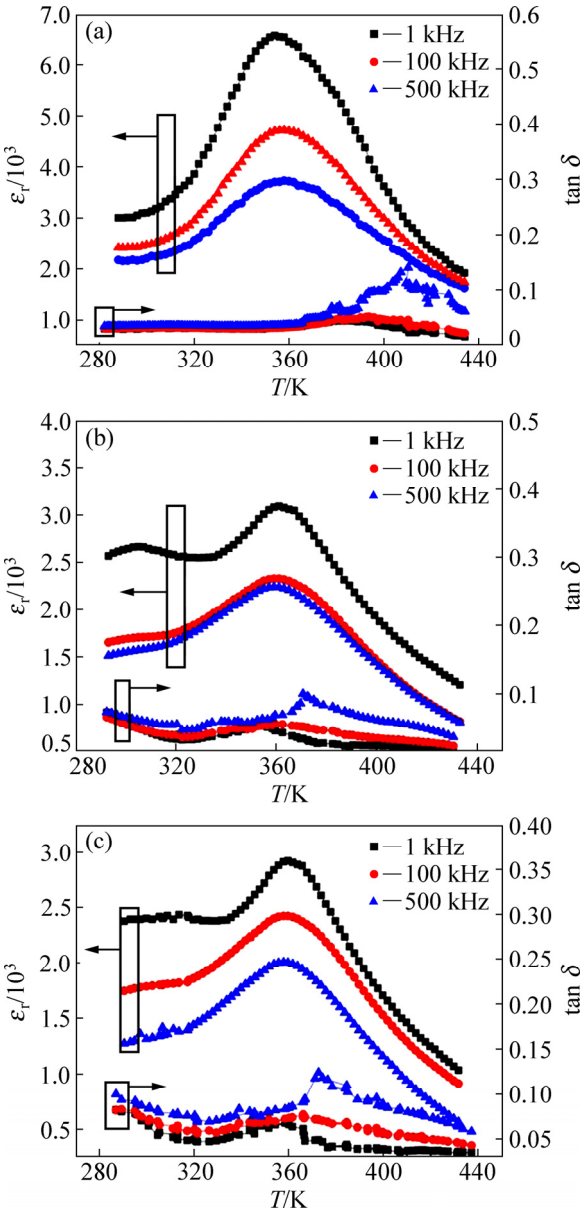

Fig. 6 Dielectric constant and loss as function of temperature under different frequencies: (a) BCZT−Sn; (b) 10% cement; (c) 15% cement

The tan δ also exhibits a well-defined peak at the transition temperature. It is interesting to note that the value of tan δ has marginally increased in cement based composites which may not affect much in electrocaloric performance.

4 Conclusions

(1) The $Ba_{0.85}Ca_{0.15}Zr_{0.1}Ti_{0.88}Sn_{0.02}O_3$−cement based composites (10% and 15% cement) were fabricated by the normal mixing and pressing method.

(2) BCZT−Sn has a saturation polarization of 17.3 μC/cm^2 which reduces to 8.20 and 6.90 μC/cm^2 for BCZT−Sn composites with 10% and 15% cement, respectively, due to decrease in density.

(3) The electrocaloric performance was evaluated using Maxwell relation and found to be adiabatic temperature changes of 0.71, 0.64 and 0.50 K and peak isothermal entropy changes of 0.86, 0.80 and 0.65 J/(kg·K) for pure sample, 10% and 15% cement composites, respectively.

(4) The dielectric constant (ε_r) at 303 K and 1 kHz is 3127 for pure BCZT−Sn ceramic and is reduced to 2614 and 2418 for 10% and 15% cement composites, respectively. It is also found that ε_r increases with the increase in BCZT−Sn content in the composites and exhibits a well-defined phase transition at 358 K.

(5) The losses in cement based composites were fairly competitive with the pristine sample. In order to confirm our findings, further studies are warranted using direct approach.

References

[1] HUANG Shi-feng, CHANG Jun, XU Rong-hua, LIU Fu-tian, LU Ling-chao, YE Zheng-mao, CHENG Xin. Piezoelectric properties of 0−3 PZT/sulfoaluminate cement composites [J]. Smart Materials and Structures, 2004, 13(2): 270−274.

[2] LI Z J, ZHANG D, WU K R. Cement-based 0−3 piezoelectric composites [J]. Journal of the American Ceramic Society, 2002, 85(2): 305−313.

[3] DONG B Q, LI Z J. Cement-based piezoelectric ceramic smart composites [J]. Composites Science and Technology, 2005, 65(9): 1363−1371.

[4] AIZAWA S, KAKIZAWA T, HIGASINO M. Case studies of smart materials for civil structures [J]. Smart Materials and Structures, 1998, 7(5): 617−626.

[5] CHAIPANICH A. Effect of PZT particle size on dielectric and piezoelectric properties of PZT−cement composites [J]. Current Applied Physics, 2007, 7(5): 574−577.

[6] CHAIPANICH A. Dielectric and piezoelectric properties of PZT−cement composites [J]. Current Applied Physics, 2007, 7(5): 537−539.

[7] LI Z J, DONG B Q, ZHANG D. Influence of polarization on properties of 0−3 cement based PZT composites [J]. Cement and Concrete Composites, 2005, 27(1): 27−32.

[8] LU Y Y, MA H Y, LI Z J. Ultrasonic monitoring of the early-age hydration of mineral admixtures incorporated concrete using cement-based piezoelectric composite sensors [J]. Journal of Intelligent Materials Systems and Structures, 2015, 26(3): 280−291.

[9] CHAIPANICH A, JAITANONG N, TUNKASIRI T. Fabrication and properties of PZT ordinary Portland cement composites [J]. Materials Letters, 2007, 61(30): 5206−5208.

[10] CHAIPANICH A, POTONG R, RIANYOI R, JAREANSUK L, JAITANONG N, YIMNIRUN R. Dielectric and ferroelectric hysteresis properties of 1−3 lead magnesium niobate−lead titanate ceramic/Portland cement composites [J]. Ceramics International, 2012, 38: s255−s258.

[11] CHAIPANICH A, JAITANONG N, YIMNIRUN R. Effect of compressive stress on the ferroelectric hysteresis behavior in 0−3 PZT−cement composites [J]. Materials Letters, 2010, 64(5): 562−564.

[12] JAITANONG N, CHAIPANICH A, TUNKASIRI T. Properties of 0−3 PZT−Portland cement composites [J]. Ceramics International, 2008, 34(4): 793−795.

[13] JAITANONG N, RIANYOI R, POTONG R, YIMNIRUN R, CHAIPANICH A. Effects of PZT content and particle size on ferroelectric hysteresis behavior of 0−3 lead zirconate titanate−Portland cement composites [J]. Integrated Ferroelectrics, 2009, 107: 43−52.

[14] HUNPRATUB S, YAMWONGB T, SRILOMSAKC S, MAENSIRID S, CHINDAPRASIRT P. Effect of particle size on the dielectric and piezoelectric properties of 0−3 BCTZO/cement composites [J]. Ceramics International, 2014, 40(1): 1209−1213.

[15] POTONG R, RIANYOI R, NGAMJARUROJANA A, CHAIPANICH A. Dielectric and piezoelectric properties of 1−3 non-lead barium zirconate titanate Portland cement composites [J]. Ceramics International, 2013, 39: s53−s57.

[16] RIANYOI R, POTONG R, NGAMJARUROJANA A, CHAIPANICH A. Influence of barium titanate content and particle size on electromechanical coupling coefficient of lead-free piezoelectric ceramic−Portland cement composites [J]. Ceramics International, 2013, 39: s47−s51.

[17] PATEL S, CHAUHAN A, VAISH R. Caloric effects in bulk lead-free ferroelectric ceramics for solid-state refrigeration [J]. Energy Technology, 2016, 4(2): 244−248.

[18] PATEL S, CHAUHAN A, VAISH R. Electric-field-driven caloric effects in ferroelectric materials for solid-state refrigeration [J]. Energy Technology, 2016, 4(3): 417−423.

[19] PATEL S, CHAUHAN A, VAISH R. Electrocaloric behavior and temperature-dependent scaling of dynamic hysteresis of $Ba_{0.85}Ca_{0.15}Ti_{0.9}Zr_{0.1}O_3$ ceramics [J]. International Journal of Applied Ceramic Technology, 2015, 12(4): 899−907.

[20] CHEN Rui, YU Sheng-wen, ZHANG Guan-jun, CHENG Jin-rong, MENG Zhong-yan. Dielectric properties of $BiFeO_3$−$PbTiO_3$ thin films prepared by PLD [J]. Transactions of Nonferrous Metals Society of China, 2006, 16: s116−s118.

[21] SAJEDEH M A, MOHAMMAD G. Electrophysical properties of ceramic−polymer composite films as function of sintering temperature [J]. Transactions of Nonferrous Metals Society of China, 2018, 28: 495−501.

[22] QIAN Xiao-shi, YE Hui-jian, ZHANG Ying-tang, GU Hai-ming, LI Xin-yu, RANDALL C A, ZHANG Q M. Giant electrocaloric response over a broad temperature range in modified $BaTiO_3$ ceramics [J]. Advanced Functional Materials, 2014, 24(9): 1300−1305.

[23] LI Ming-ding, TANG Xin-gui, ZENG Si-ming, LIU Qiu-xiang, JIANG Yan-ping, ZHANG Tian-fu, LI Wen-hua. Large electrocaloric effect in lead-free $Ba(Hf_xTi_{1-x})O_3$ ferroelectric ceramics for clean energy applications [J]. ACS Sustainable Chemistry & Engineering, 2018, 6(7): 8920−8925.

[24] KIM Y S, YOO J. Electrocaloric effect of lead-free $(Ba,Ca)(Zr,Ti)O_3$ ferroelectric ceramic [J]. Journal of Electronic Materials, 2015, 44(8): 2555−2558.

[25] TIAN Yong-shang, GONG Yan-sheng, MENG Da-wei, DENG Hao, KUANG Bo-ya. Low temperature sintering and electric properties of BCT−BZT and BCZT lead-free ceramics [J]. Journal of Materials

Science: Materials in Electronics, 2015, 26(6): 3750−3756.
[26] PATEL S, CHAUHAN A, VAISH R. Multiple caloric effects in $(Ba_{0.865}Ca_{0.135}Zr_{0.1089}Ti_{0.8811}Fe_{0.01})O_3$ ferroelectric ceramic [J]. Applied Physics Letters, 2015, 107(4): 042902.
[27] KADDOUSSI H, LAHMARA A, GAGOUA Y, DELLISA J L, KHEMAKHEMB H, MARSSIA M E L. Electro-caloric effect in lead-free ferroelectric $Ba_{1-x}Ca_x(Zr_{0.1}Ti_{0.9})_{0.925}Sn_{0.075}O_3$ ceramics [J]. Ceramics International, 2015, 41(10): 15103−15110.
[28] KADDOUSSI H, GAGOU Y, LAHMAR A, BELHADI J, ALLOUCHE B, DELLIS J L, COURTY M, KHEMAKHEM H, MARSSI M E L. Room temperature electro-caloric effect in lead-free $Ba(Zr_{0.1}Ti_{0.9})_{1-x}Sn_xO_3$ (x=0, 0.075) ceramics [J]. Solid State Communications, 2015, 201: 64−67.
[29] PATEL S, SHARMA P, VAISH R. Enhanced electrocaloric effect in $Ba_{0.85}Ca_{0.15}Zr_{0.1}Ti_{0.9-x}Sn_xO_3$ ferroelectric ceramics [J]. Phase Transitions, 2016, 89(11): 1062−1073.
[30] SRIKANTH K S, SATYANARAYAN P, RAHUL V. Functional cementitious composites for pyroelectric applications [J]. Journal of Electronic Materials, 2017, 47(4): 2378−2385.
[31] CHAIPANICH A, ZENG H R, LI G R, YIN Q R, YIMNIRUN R, JAITANONG N. Piezoelectric force microscope investigation and ferroelectric hysteresis behavior of high volume piezoelectric ceramic in 0−3 lead zirconate titanate−cement composites [J]. Ferroelectrics, 2016, 492(1): 54−58.
[32] CHAIPANICH A, JAITANONG N, YIMNIRUN R. Effect of carbon addition on the ferroelectric hysteresis properties of lead zirconate−titanate ceramic−cement composites [J]. Ceramics International, 2011, 37(4): 1181−1184.
[33] HUANG S F, HUANG S F, CHANG J, LU L C, LIU F T, YE Z M, CHENG X. Preparation and polarization of 0−3 cement based piezoelectric composites [J]. Materials Research Bulletin, 2006, 41(2): 291−297.
[34] HUANG S F, LU L C, JUN C, XU D Y, LIU F T, XIN C. Influence of ceramic particle size on piezoelectric properties of cement-based piezoelectric composites [J]. Ferroelectrics, 2006, 332: 187−194.
[35] POTONG R, RIANYOI R, JAITANONG N, YIMNIRUN R, CHAIPANICH A. Ferroelectric hysteresis behavior and dielectric properties of 1−3 lead zirconate titanate−cement composites [J]. Ceramics International, 2012, 38: s267−s270.
[36] SATYANARAYAN P, ADITYA C, SWARUP K, NIYAZ A M, BOURAOUI I, R VAISH K B R V. Tuning of dielectric, pyroelectric and ferroelectric properties of $0.715Bi_{0.5}Na_{0.5}TiO_3$−$0.065BaTiO_3$−$0.22SrTiO_3$ ceramic by internal clamping [J]. AIP Advances, 2015, 5: 087145.
[37] HAO Ji-gong, BAI Wang-feng, LI Wei, ZHAI Ji-wei. Correlation between the microstructure and electrical properties in high-performance $(Ba_{0.85}Ca_{0.15})(Zr_{0.1}Ti_{0.9})O_3$ lead-free piezoelectric ceramics [J]. Journal of the American Ceramic Society, 2012, 95(6): 1998−2006.
[38] WU Jia-gang, XIAO Ding-quan, WU Bo, WU Wen-juan, ZHU Jian-guo, YANG Zheng-chun, JOHN Wang. Sintering temperature-induced electrical properties of $(Ba_{0.90}Ca_{0.10})(Ti_{0.85}Zr_{0.15})O_3$ lead-free ceramics [J]. Materials Research Bulletin, 2012, 47(5): 1281−1284.
[39] SINGH G, BHAUMIK I, GANESAMOORTHY S, BHATT R, KARNAL A K, TIWARI V S, GUPTA P K. Electro-caloric effect in $0.45BaZr_{0.2}Ti_{0.8}O_3$−$0.55Ba_{0.7}Ca_{0.3}TiO_3$ single crystal [J]. Applied Physics Letters, 2013, 102(8): 082902.
[40] SINGH G, TIWARI V S, GUPTA P K. Electro-caloric effect in $(Ba_{1-x}Ca_x)(Zr_{0.05}Ti_{0.95})O_3$: A lead-free ferroelectric material [J]. Applied Physics Letters, 2013, 103(20): 202903.
[41] BAI Yang, HAN Xi, DING Kai, QIAO Li-jie. Combined effects of diffuse phase transition and microstructure on the electrocaloric effect in $Ba_{1-x}Sr_xTiO_3$ ceramics [J]. Applied Physics Letters, 2013, 103(16): 162902.

$Ba_{0.85}Ca_{0.15}Zr_{0.1}Ti_{0.88}Sn_{0.02}O_3$−水泥复合材料的电热行为

P. SURESH, P. MATHIYALAGAN, K. S. SRIKANTH

School of Mechanical Engineering, Galgotias University, Greater Noida, Uttar Pradesh, 201306, India

摘　要：寻找用于土木工程结构的多功能材料的努力引起全球研究人员的兴趣。在不同 $Ba_{0.85}Ca_{0.15}Zr_{0.1}$-$Ti_{0.88}Sn_{0.02}O_3$(BCZT−Sn)与水泥配比条件下，制备适合于电热应用的水泥基 BCZT−Sn 复合材料。水泥基复合材料的磁滞回线表现出一定的饱和特征，纯 BCZT−Sn 样品的磁滞回线则由于其铁电性质而饱和。此外，首次探索这种复合材料在固态制冷技术中的应用，即其电热效应(ECE)。在 0~29 kV/cm 的电场作用下，纯 BCZT−Sn、含 10%水泥及 15%水泥的复合材料的热力学温度变化分别为 0.71、0.64 和 0.50 K，等温熵变分别为 0.86、0.80 和 0.65 J/(kg·K)。水泥基复合材料的热力学温度变化与 BCZT−Sn 铁电陶瓷的相当。此外，具有不同陶瓷含量的复合材料的室温介电常数(ε_r)数随着复合材料中 BCZT−Sn 含量的增加而增大。由于其优异的性能，这种水泥基 BCZT−Sn 复合材料有望用于固态制冷技术中。

关键词：电热行为；水泥基复合材料；介电；熵

(Edited by Wei-ping CHEN)